Exendin-4 inhibits lipotoxicity-induced oxidative stress in β-cells by inhibiting the activation of TLR4/NF-κB signaling pathway

XIMEI SHEN[1,2*], LIUFEN LUO[1*], MENG YANG[1*], YUXI LIN[1], JING LI[1] and LIYONG YANG[1,2]

[1]Endocrinology Department, The First Affiliated Hospital of Fujian Medical University;
[2]Diabetes Research Institute of Fujian Province, Fuzhou, Fujian 350005, P.R. China

Received May 29, 2019; Accepted December 2, 2019

DOI: 10.3892/ijmm.2020.4490

Abstract. The present study aimed to investigate the relationship between the protective effects of exendin-4 (EX-4) on lipotoxicity-induced oxidative stress and meta-inflammation in β-cells and the toll-like receptor 4 (TLR4)/NF-κB signaling pathway. Lipotoxicity, hydrogen peroxide (H_2O_2)-induced oxidative stress in β cells, obese Sprague Dawley rats and TLR4 truncation rats were utilized in the present study. The expression levels were detected by western blotting; cell apoptosis was detected by TUNEL assay; and the intracellular reactive oxygen species (ROS) levels were analyzed using a ROS assay kit. The findings of the present study showed that EX-4 inhibited the expression of TLR4, NF-κB p65 subunit and $p47^{phox}$ in a concentration-dependent manner, and decreased the intracellular level of ROS. Additionally, silencing of TLR4 expression enhanced the protective effects of EX-4, while overexpression of TLR4 attenuated these protective influences. Simultaneously, it was demonstrated that TLR4 was involved in the process of EX-4 intervention to inhibit H_2O_2-induced oxidative stress in islet β-cells. Moreover, it was found that EX-4 also inhibited TLR4- or NF-κB agonist-induced oxidative stress. These results were also confirmed in an animal model of obese rats, in which EX-4 was able to improve the function of β-cells, attenuate oxidative stress, and inhibit the expression levels of TLR4 and NF-κB p65 subunit in the pancreas of the diet-induced obese rats. Furthermore, truncation of the TLR4 gene in SD rats delayed the aforementioned damage. In summary, EX-4 may inhibit lipotoxicity-induced oxidative stress in β-cells by inhibiting the activation of the TLR4/NF-κB signaling pathway.

Correspondence to: Dr Liyong Yang, Endocrinology Department, The First Affiliated Hospital of Fujian Medical University, 20 Chazhong Road, Fuzhou, Fujian 350005, P.R. China
E-mail: liyongy@medmail.com.cn

*Contributed equally

Key words: exendin-4, lipotoxicity, meta-inflammation, toll-like receptor 4, oxidative stress

Introduction

Exendin-4 (EX-4) is widely used for the treatment of type 2 diabetes worldwide (1). There is an increasing evidence that EX-4 has multiple influences on β-cells (2-4). EX-4 not only promotes the proliferation of β-cells (5) and insulin secretion (6), suppresses appetite (7) and reduces body weight (BW) (8), but also has additional protective effects, such as inhibiting inflammation (9,10), protecting cardiomyocytes via improvement of mitochondrial function (11) and improving non-alcoholic steatohepatitis by regulating hepatic fatty acid metabolism (12). Therefore, it is important to further explore the other protective effects of EX-4.

At present, metabolic inflammatory injury is considered as an important mechanism in lipotoxicity-induced β-cell apoptosis; however, no targeted interventions have yet been developed. It is well known that toll-like receptor 4 (TLR4) is a key factor in the innate immune activation of the inflammatory signaling pathway, acting as an important mediator of lipotoxicity-induced inflammation (13). To date, TLR4 has been confirmed to be expressed in β-cells (14). A previous study showed that overactivation of TLR4 induces oxidative stress and leads to dysfunction in insulin secretion (15). Previous experiments demonstrated that lipotoxicity directly activates the TLR4-JNK signaling pathway and increases oxidative stress in islet β-cells, inducing insulin secretion and apoptosis in β-cells (16). A previous study demonstrated that inhibition of TLR4 could mitigate the damage caused by oxidative stress in cardiomyocytes (17), the liver (18) and the kidneys (19). However, whether inhibition of TLR4 activity in β-cells is beneficial for inhibiting lipotoxicity-induced oxidative stress in β-cells requires further exploration.

A number of scholars reported that EX-4 protects β-cells from lipotoxicity (20) and inhibits lipotoxicity-induced oxidative stress in β-cells (21). However, whether the protective effects of EX-4 on β-cells are related to the inhibition of metabolic inflammation by TLR4 signaling has not yet been elucidated. In addition, it has been confirmed that EX-4 has an inhibitory effect on TLR4 and oxidative stress in other systems. For example, Yang *et al* (22) reported the beneficial influences of EX-4 on blood vessels, which were partially attributed to the inhibition of oxidative stress and inflammation. Besides, it has been suggested that the anti-inflammatory effect of EX-4 is related to TLR4.

The present study aimed to explore the relationship between the protective effects of EX-4 on lipotoxicity-induced oxidative stress via the TLR4/NF-κB signaling pathway in β-cells, by using βTC6 cells, high-fat diet-induced obese rats and TLR4 truncation rats as subjects. For the first time, to the best of our knowledge, it was reported that EX-4 inhibited apoptosis, dysfunction and lipotoxicity-induced oxidative stress in β-cells by inhibiting metabolic and inflammatory pathways.

Materials and methods

Cell culture. The mouse islet cell line βTC6 (American Type Culture Collection) was cultured in DMEM (4.5 g/l glucose; Gibco; Thermo Fisher Scientific, Inc.), supplemented with 10% FBS (Gibco; Thermo Fisher Scientific, Inc.), 2 mmol/l L-glutamine, 10 mmol/l HEPES, 100 U/ml penicillin and 100 μg/ml streptomycin (complete medium). Cells were incubated in the presence of 5% CO_2 at 37˚C. According to the growth of the cells and the pH value of the medium, the medium was changed once every 1-2 days. Cells at passages 15-18 were used for further experiments. The cells were seeded at a density of $3x10^5$ cells/ml.

Cell intervention

Preparation of medium for treatment with palmitic acid (PA). Referring to the method described by Ke *et al* (23), the process was as follows: 512 mg PA (Sigma-Aldrich; Merck KGaA; molecular mass, 256.42) was dissolved in 10 ml absolute ethanol, and then titrated with 0.1 mol/l NaOH (10 ml) at 70˚C. After that, 10 ml PA mixture was added to 190 ml 10% BSA (Sigma-Aldrich; Merck KGaA) at 55˚C to form a complex at a concentration of 5 mmol/l. The stock solution was filter-sterilized and stored at -20˚C. A control solution, containing 5% ethanol and 9.5% BSA, was similarly prepared.

PA or H_2O_2 intervention. βTC6 cells were cultured in 6-well plates for 24 h after reaching 50% confluence. The cell culture medium was removed, and the cells were washed twice with PBS and then treated with 0.5 mmol/l PA (Sigma-Aldrich; Merck KGaA) or 100 μmol/l H_2O_2 with complete medium for 24 h. Cells were treated with BSA/ethanol in complete medium without PA for 24 h as controls (Fig. S1).

EX-4 intervention. In the current study, βTC6 cells were treated with 0.5 mmol/l PA or 100 μmol/l H_2O_2 for 24 h, and then exposed to different concentrations (25, 50 and 100 nmol/l) of EX-4 with complete medium [dissolved in 0.1% DMSO (v/v); ProSpec-Tany TechnoGene, Ltd.] for 72 h. PA-induced or H_2O_2-induced cells without EX-4, and non-induced cells exposed to EX-4, were used as controls.

Protein agonist intervention. In the present study, βTC6 cells were pretreated with 10 mg/l TLR4 agonist [lipopolysaccharide (LPS), dissolved in 0.1% DMSO (v/v); Sigma-Aldrich; Merck KGaA) or 50 nmol/l NF-κB agonist [tumor necrosis factor-α (TNF-α), dissolved in 0.1% DMSO (v/v); Sigma-Aldrich; Merck KGaA] for 24 h before being exposed to 100 nmol/l EX-4 with complete medium for 72 h. Cells exposed to LPS, TNF-α or complete medium alone were used as controls.

TLR4 small interfering (si)RNA and TLR4 cloning in βTC6 cells. Silencing with TLR4 siRNA was performed based on a previously described method (16). The GV492 vector carrying mouse TLR4 cDNA was supplied by Shanghai GenePharma Co., Ltd. The primers used for the synthesis of TLR4 cDNA were as follows: TLR4 (24379-1)-P1 (5'-3'), AGGTCGACT CTAGAGGATCCCGCCACCATGATGCCTCCCTGGCTC CTGGCTAGG; and TLR4 (24379-1)-P2 (5'-3'), TCCTTG TAGTCCATACCGGTCCAAGTTGCCGTTTCTTGTTC TTC (the PCR results are shown in Fig. S2). The cells were seeded at a density of $3x10^5$ cells/ml. The RNAi lentiviral vector or TLR4-expressing lentiviral vector was diluted to $1x10^8$ IU/ml, and then directly diluted in DMEM + 10% FBS with 2 mmol/L L-glutamine at a multiplicity of infection (MOI) of 50. After 10-12 h of incubation in the presence of 5% CO_2 at 37˚C, the transduction medium (the 50 MOI viral solution + DMEM + 10% FBS + 2 mmol/l L-glutamine) was replaced with fresh complete medium (DMEM + 10% FBS + 2 mmol/l L-glutamine), and then the cells were incubated for 72 h. The expression level of TLR4 was detected by western blotting.

Glucose-stimulated insulin secretion. According to a previously described method (16), the treated βTC6 cells were washed twice with glucose-free Krebs-Ringer bicarbonate buffer (KRBB, pH 7.4; KCl 4.8 mmol/l, KH_2PO_4 1.2 mmol/l, NaCl 129.0 mmol/l, $NaHCO_3$ 5.0 mmol/l, $CaCl_2$ 1.0 mmol/l, $MgSO_4$ 1.2 mmol/l, HEPES 10.0 mmol/l, BSA 0.1%) and preincubated at 37˚C for 30 min with glucose-free KRBB. Cells were then washed once with glucose-free KRBB, and incubated for 60 min at 37˚C in KRBB containing 5.6 or 20 mmol/l glucose. Aliquots of supernatant were collected and assessed using an ELISA kit (Cusabio Technology, LLC; cat. no. P01325).

Animal experiments. A total of 30 specific pathogen-free-grade male Sprague-Dawley (SD) rats (5-6 weeks old; weighing 220±10 g; Animal Experimental Center of Fujian Medical University, Fujian, China) and 30 male TLR4 truncation SD rats (CRISPR/Cas9 gene targeting; 5-6 weeks old; weighing 220±10 g; $TLR4^{trun/trun}$, Shanghai GenePharma Co., Ltd.) were randomly selected. Construction of the TLR4 truncation rats is described in Data S1. The rats had free access to food and water during the whole experimental period. The rats were housed in an intelligent artificial climate box (RXZ-380C; Ningbo Jiangnan Instrument Factory) with the temperature maintained at 20-25˚C, a 12/12 h light/dark cycle, and a relative humidity of 55±5%. SD rats and $TLR4^{trun/trun}$ rats were randomly divided into a normal diet group (n=10) and a high-fat diet (HFD) group (n=20). The HFD included 60% of the calories from fat, 20% of the calories from protein and 20% of the calories from carbohydrate (Research Diets, Inc.; cat. no. D12492; ingredients listed in Table SI). The HFD group was randomly divided into two subgroups after 16 weeks; one group was subcutaneously given exenatide (EXE) at a dose of 5 μg/kg·day and another group was subcutaneously given the same amount of normal saline for 16 weeks. Additionally, BW and body length (BL) were recorded weekly during the study and Lee's index was calculated according to the following formula: $\sqrt[3]{BW(g) \times 1000}$/BL (cm).

The study was approved by the Biomedical Research Ethics Committee of the First Affiliated Hospital of Fujian Medical University.

Testing of biochemical indicators. The control and experimental rats were euthanized, and the abdominal aorta blood was collected and centrifuged in 1,500 x g for 10 min at room temperature after being maintained at room temperature for 30 min. The serum was then stored in a refrigerator at -80˚C for further analysis. The levels of insulin and free fatty acid (FFA) were detected by ELISA (Cusabio Technology, LLC; cat. no. PQ8BM4E6), and the levels of fasting blood glucose (FBG), total cholesterol (TCHO), triglyceride (TG) and low-density lipoprotein (LDL) were measured using an automatic biochemical analyzer, according to a previously described method (16). Homeostatic model assessment of insulin resistance (HOMA-IR) was calculated as follows: (FBG x fasting blood insulin)/22.5.

Analysis of apoptosis by TUNEL assay

Detection of apoptosis of βTC6 cells. The TUNEL assay was undertaken using a dead-End™ Fluorometric TUNEL System (Promega Corporation). Paraformaldehyde solution (4%; pH 7.4) was used for fixing at 4˚C for 30 min. In addition, both apoptotic and non-apoptotic cells were stained red with PI. Fluorescein-12-dUTP (10 μg/ml; incubated at 37˚C for 60 min) incorporation resulted in localized green fluorescence within the nucleus of apoptotic cells only. PI was used at a concentration of 1 μg/ml, and incubated for 30 min at room temperature. Since the PI dye also binds to RNA at the same time, the cells were digested with RNase (50 units of RNase for 15 min at 37˚C or 30 min at room temperature) before PI staining. The detection of apoptosis of islet β-cell by flow cytometry in rats was performed according to previously described methods (24).

Detection of apoptosis of pancreatic tissues. Pancreatic tail tissue sections were fixed in 4% paraformaldehyde (pH 7.4) for 24 h at room temperature and paraffin-embedded. Sections were dewaxed according to a conventional method: Sections with a thickness of 4 μm were immersed in xylene twice for 5 min, and then were soaked in 100, 95, 85 and 70% ethanol for 5 min, followed by PBS three times for 3 min. After permeabilization, the sections were washed with 3% H_2O_2-methanol solution for 15 min. Afterwards, prepared proteinase K (100 μl) was added into each sample and reacted at 37˚C for 30 min, followed by the addition of 100 μl of fluorescein isothiocyanate (FITC)-labeled streptavidin (FITC-SA) solution to each sample. The reaction was incubated at 37˚C for 1 h in the dark, followed by washing, counterstaining with 100 μl (DAPI; 3 μg/ml) and further washing at room temperature. Finally, the samples were observed by fluorescence microscopy (10x40 magnification).

Protein extraction and western blotting

Protein extraction. Whole-cell and nuclear extracts were prepared for western blot analysis (25). Islets were isolated from the pancreas of each SD rat (26). The cells and pancreatic tissues were added to RIPA buffer (Beyotime Institute of Biotechnology), containing 1 mmol/l PMSF, and lysed on ice for 30 min. The cells and tissues were centrifuged at 12,900 x g for 10 min at 4˚C, the supernatant was transferred to a new EP tube, 15 μl supernatant was left for the determination of protein concentration, and the remainder was mixed with 5X SDS-PAGE sample loading buffer. The protein was thoroughly denatured in a 95-100˚C water bath for 5 min and then stored at -20˚C.

Western blotting. The protein concentration was detected by BCA assay. SDS-PAGE analysis of proteins before and after treatment with 50 mM DTT was performed on a 4-10% gradient gel containing 0.1% SDS (Laemmli system). Preparations of the proteins (30 μg) were incubated in a buffer containing 50 mM Tris-HCl (pH 6.8), 1% SDS, 10% glycerol, 0.001% bromophenol blue and 10 mM EDTA, with or without 50 mM DTT, for 16 min at 100˚C, and then applied to the gel. Then the protein sample was transferred onto a PVDF membrane (Invitrogen; Thermo Fisher Scientific, Inc.). TBS was transferred into the upper membrane, and blocking solution (skimmed milk; 5%; Beijing Dingguo Changsheng Biotechnology Co., Ltd.) was then added into the wet PVDF membrane for 1 h at room temperature. After that, anti-TLR4 (1:1,000; Abcam; cat. no. ab13556), anti-NF-κB p65 (1:1,000; Cell Signaling Technology, Inc.; cat. no. 8242), anti-P47 phox (1:200; Santa Cruz Biotechnology, Inc.; cat. no. NB100-790), anti-GAPDH antibody (1:3,000; Abcam; cat. no. EPR1689) or anti-β-actin (1:200; Santa Cruz Biotechnology, Inc.; cat. no. 932715) were added, and then incubated at 4˚C overnight. The membrane was incubated with horseradish peroxidase-labeled secondary antibody (1:5,000; Beijing Dingguo Changsheng Biotechnology Co., Ltd.; cat. no. IH-0011) for 1 h at room temperature. The gel was visualized and analyzed using JESS (ProteinSimple) and the images were then saved.

Detection of reactive oxygen species (ROS). βTC6 cells and frozen sections of pancreatic tissues were assessed using a ROS assay kit (Beyotime Institute of Biotechnology). The βTC6 cells or pancreatic tissues were incubated in 10 μmol/l dichloro-dihydro-fluorescein diacetate for 20 min at 37˚C in 5% CO_2. Confocal laser scanning microscopy was used to directly observe the intracellular ROS levels as described previously (27).

Immunofluorescence. Each group of pancreatic paraffin-embedded sections was dewaxed according to a conventional method, hydrated, and then the sections with a thickness of 4 μm were immersed in xylene twice for 5 min. The sections were then soaked in 100, 95, 85 and 70% ethanol for 5 min, followed by PBS three times for 3 min, and heat-induced antigen retrieval (HIAR) was performed. HIAR was carried out in citrate buffer (pH 6) at 120˚C for 15 min in the Rapid Microwave Histoprocessor Histos Pro (Milestone Medical). To each section, 3% H_2O_2-methanol solution was added for 10 min, and then the sections were blocked with 50-100 μl goat serum (Gibco; Thermo Fisher Scientific, Inc.; cat. no. 16210064 for 20 min at room temperature. The sections were incubated with 50-100 μl primary antibody (1:50) [anti-TLR4 (Abcam; cat. no. ab13556), anti-NF-κB p65 (Cell Signaling Technology, Inc.; cat. no. 8242), anti-$p47^{phox}$ (Santa Cruz Biotechnology, Inc.; cat. no. NB100-790), anti-GAPDH

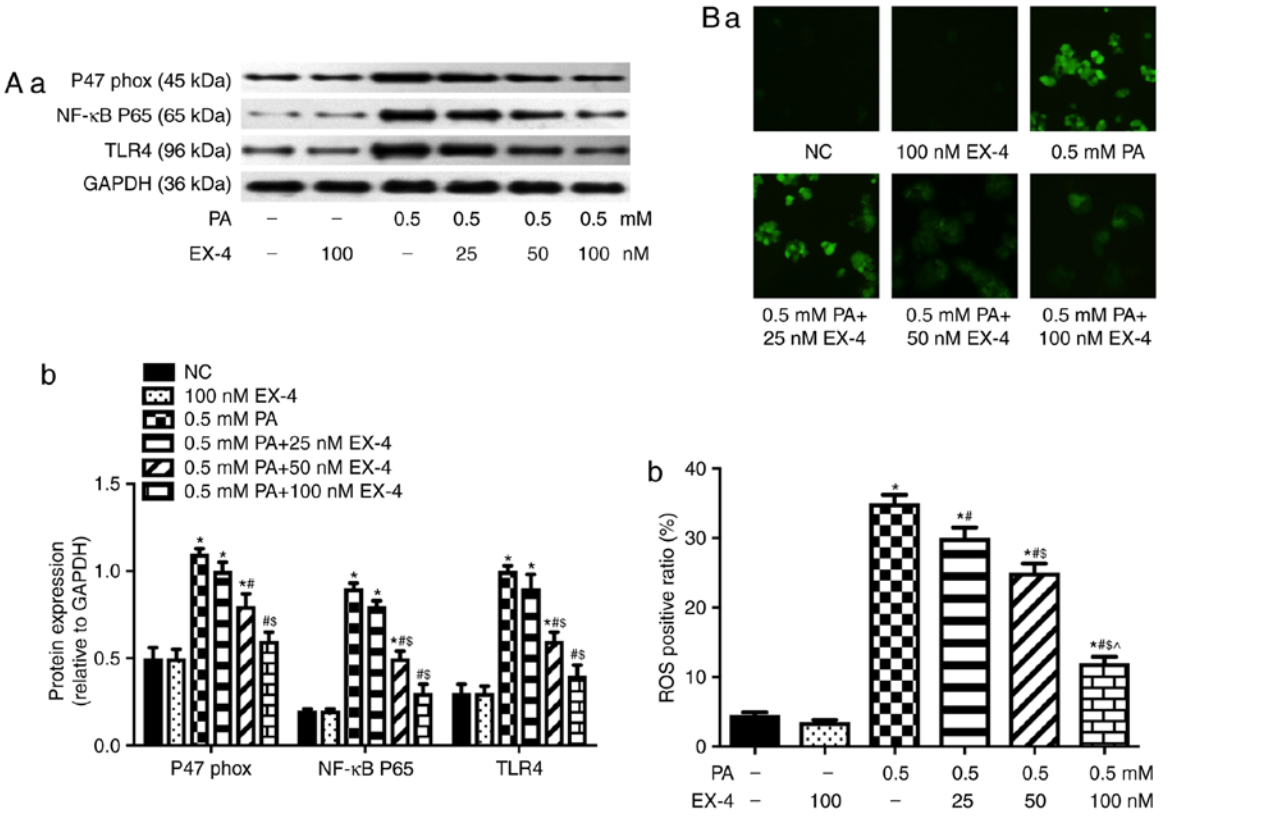

Figure 1. EX-4 inhibits PA-induced oxidative stress in β-cells and the expression levels of TLR4 and NF-κB p65 subunit in a dose-dependent manner. (A) Western blotting was performed to detect the expression levels of $p47^{phox}$, TLR4 and NF-κB p65 subunit. (A-a) Representative western blot images in each group. (A-b) The ratio of target protein to GAPDH. (B) EX-4 reduced the PA-induced ROS positive ratio in β-cells. (B-a) Representative images from fluorescent microscopy in each group. (B-b) The collective analyses of all three independent experiments. *P<0.05 vs. NC group (without PA and EX-4), $^{\#}$P<0.05 vs. 0.5 mM PA group, $^{\$}$P<0.05 vs. 0.5 mM PA + 25 nM EX-4 group, $^{\wedge}$P<0.05 vs. 0.5 mM PA + 50 nM EX-4 group. Magnification, x40. EX-4, exendin-4; PA, palmitic acid; ROS, reactive oxygen species; NC, negative control; TLR4, toll-like receptor 4.

(Abcam; cat. no. EPR1689) or anti-β-actin (Santa Cruz Biotechnology, Inc.; cat. no. 932715)] for 2 h at 37˚C in a wet box. This was followed by incubation of the sections with 50-100 μl secondary antibody conjugated to FITC/TRITC (1:200; Abcam; cat. no. ab6785.) for 1 h at 37˚C in the dark. Each slice was incubated in 50-100 μl DAPI solution for 5 min at room temperature in the dark, and then sealed with anti-extraction sealant. The expression levels in the cells were observed under a fluorescence microscope (x40 magnification), and the three expression regions were photographed and stored (Olympus CKX53; Olympus Corporation).

RNA extraction and reverse transcription-semiquantitative PCR (RT-sqPCR). Total RNA was extracted from animal tissues using the TRIzol® reagent (Thermo Fisher Scientific, Inc.) method. The RNA was reverse transcribed into cDNA using a PrimeScript™ RT reagent kit (Takara Bio, Inc.) in a 10-μl RT reaction system, at 37˚C for 15 min and 85˚C for 5 sec. A total of 2 μl cDNA was taken for the PCR amplification in a 25-μl PCR reaction system (Invitrogen; Thermo Fisher Scientific, Inc.). The reaction parameters were 95˚C for 5 min, 95˚C for 30 sec, 56.5˚C for 30 sec and 72˚C for 30 sec for 35 cycles, and finally extended to 72˚C for 10 min. β-actin was used as an internal reference for the PCR reaction. The sequences of primers were as follows: TLR4 forward primer, 5'-AGTGCTTGTGTGGTAGAGGCAA-3'; TLR4 reverse primer, 5'-CTGCCTACCAAATAGAAACCAGG-3'; β-actin forward primer, 5'-CACCCGCGAGTACAACCTTC-3'; and β-actin reverse primer, 5'-CCCATACCCACCATCACACC-3'. Next, the PCR products (5 μl/lane) were analyzed by electrophoresis on 1.5% agarose gels (with 2.5 μl ethidium bromide) for 30 min at 160 mV. The electrophoresis results were collected using a computer gel scanning imaging system and analyzed by Image Lab software 3.0 (Bio-Rad Laboratories, Inc.).

Statistical analysis. Statistical analysis was performed using SPSS 20.0 software (IBM Corp.). The results are expressed as the mean ± SEM of three independent experiments. One-way ANOVA was used in a completely randomized design. The Bonferroni test was undertaken to make comparisons between each two groups. To control for the effects of blood glucose, covariance analysis was used to investigate the effect of EXE on animal experiments (Table SII). P<0.05 was considered to indicate a statistically significant difference.

Results

EX-4 inhibits oxidative stress in PA-induced β-cells and the expression levels of TLR4 and NF-κB p65 subunit. A previous study showed that EX-4 improved lipotoxicity-induced apoptosis and insulin secretion (28). According to a previously described method, the present study observed the effects of EX-4 on lipotoxicity-induced oxidative stress in β-cells, and the expression levels of TLR4 and NF-κB p65 subunit. The

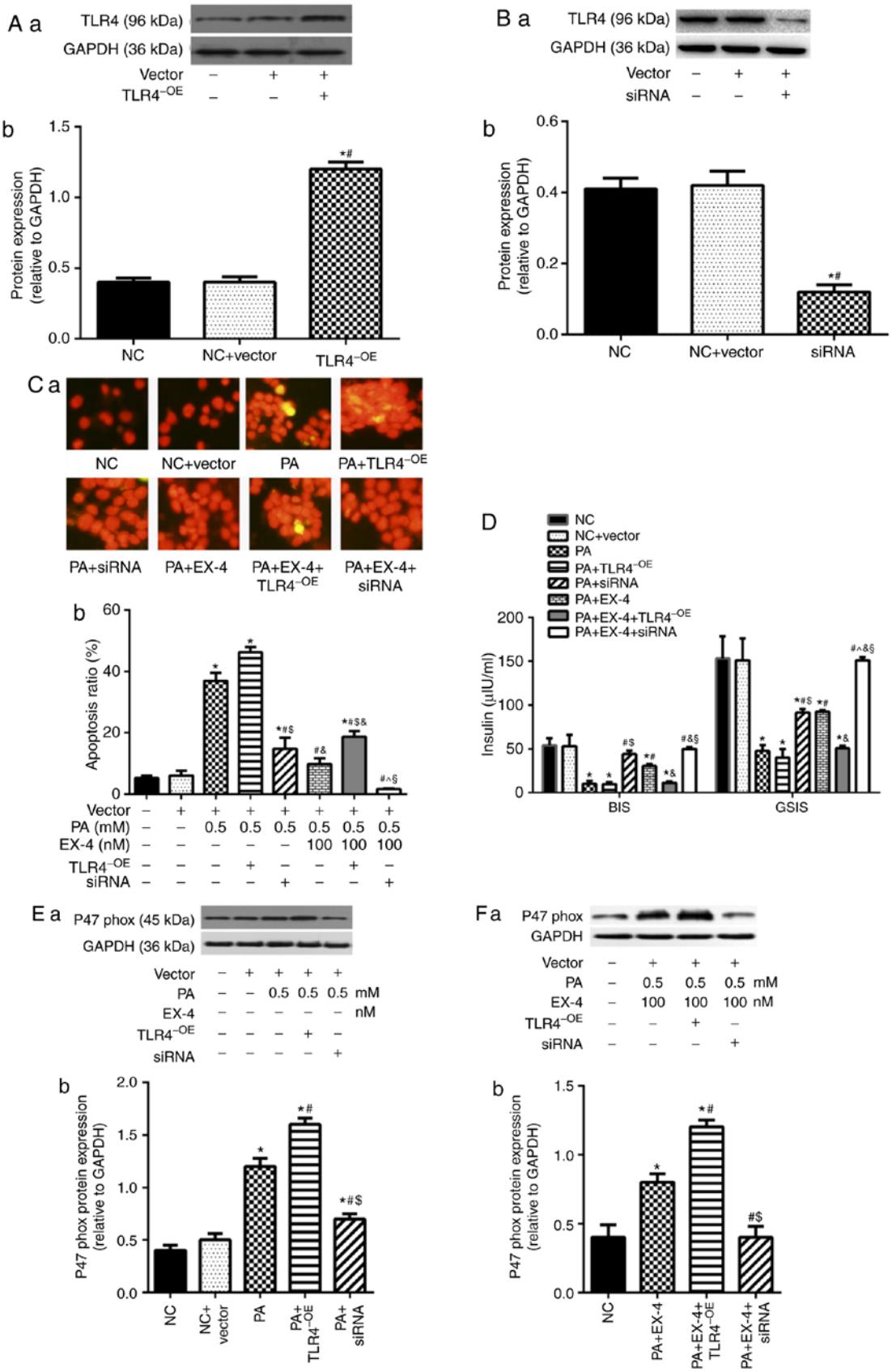

Figure 2. Regulation of TLR4 expression alters the protective effects of EX-4 in PA-induced β-cells. Expression levels of TLR4 were detected by western blotting in (A) TLR4-overexpressing and (B) siRNA-transfected cells. (A-a and B-a) Representative western blot images in each group. (A-b and B-b) The ratio of target protein to GAPDH. *P<0.05 vs. NC group, #P<0.05 vs. NC + Vector group. (C) Apoptosis rate of β-cells. (C-a) Representative images from fluorescent microscopy in each group. (C-b) The collective analyses of all three independent experiments. (D) Insulin secretion. *P<0.05 vs. NC group, #P<0.05 vs. 0.5 PA group, $P<0.05 vs. 0.5 PA + TLR4-OE group, ^P<0.05 vs. 0.5 PA + siRNA group, &P<0.05 vs. PA + 100 EX-4 group, §P<0.05 vs. PA + EX-4 + TLR4-OE group. Expression level of $p47^{phox}$ in (E) TLR4-overexpressing cells. (E-a) Representative western blot images in each group. (E-b) The ratio of target protein to GAPDH. *P<0.05 vs. NC group, #P<0.05 vs. 0.5 PA group, $P<0.05 vs. PA + TLR4-OE group. Expression level of $p47^{phox}$ in (F) siRNA-transfected cells. (F-a) Representative western blot images in each group. (F-b) The ratio of target protein to GAPDH. *P<0.05 vs. NC group, #P<0.05 vs. PA + EX-4 group, $P<0.05 vs. PA + EX-4 + TLR4-OE group.

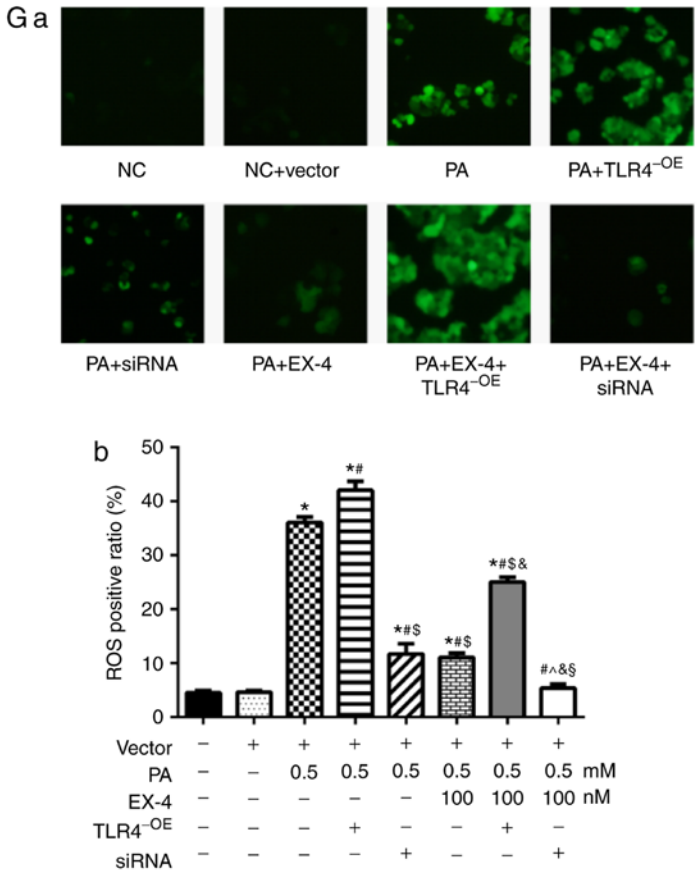

Figure 2. Continued. (G) ROS in β-cells was detected by immunofluorescence. (G-a) Representative images from fluorescent microscopy in each group. (G-b) The collective analyses of all three independent experiments. *P<0.05 vs. NC group, #P<0.05 vs. 0.5 PA group, $P<0.05 vs. 0.5 PA + TLR4-OE group, ^P<0.05 vs. 0.5 PA + siRNA group, &P<0.05 vs. PA + 100 EX-4 group, §P<0.05 vs. PA + EX-4 + TLR4-OE group. Magnification, x40. EX-4, exendin-4; PA, palmitic acid; OE, overexpression; NC, negative control; siRNA, small interfering RNA; TLR4, toll-like receptor 4; BIS, basal insulin secretion; GSIS, glucose-stimulated insulin secretion.

results of the present study revealed that EX-4 inhibited the expression levels of TLR4 and NF-κB p65 subunit (Fig. 1A) in a concentration-dependent manner, inhibiting the expression of $p47^{phox}$ (Fig. 1A) and decreasing the intracellular level of ROS (Fig. 1B).

Regulation of TLR4 expression alters the protective effects of EX-4 on lipotoxicity-induced oxidative stress in β-cells. The aforementioned experiments showed that EX-4 can inhibit oxidative stress in β-cells and decrease the expression levels of TLR4 and NF-κB p65 subunit. Therefore, the present study further assessed whether TLR4 could be involved in the protective effects of EX-4 by lentivirus-mediated overexpression (Fig. 2A) or silencing (Fig. 2B) of TLR4 in β-cells. The results demonstrated that upregulation of TLR4 attenuated the effect of EX-4 on lipotoxicity-induced β-cell apoptosis (Fig. 2C), insulin secretion (Fig. 2D) and oxidative stress (Fig. 2E-G), and the opposite was observed when the expression of TLR4 was inhibited (Fig. 2C-G).

TLR4 is involved in the role of EX-4 in attenuating H_2O_2-induced oxidative stress in β-cells. The previous two parts of the study confirmed that EX-4 was involved in the inhibition of oxidative stress in β-cells. To further confirm the specificity of this process, H_2O_2 was used to induce oxidative stress in β-cells, followed by intervention with EX-4. The findings demonstrated that EX-4 reduced H_2O_2-induced apoptosis (Fig. 3A), increased insulin secretion (Fig. 3B) and inhibited oxidative stress (Fig. 3C and D) in β-cells.

Simultaneously, lentivirus-mediated overexpression or silencing of TLR4 was used to verify the influences of TLR4 expression on the treatment with EX-4 in H_2O_2-induced β-cells. The results showed that up-regulation of TLR4 attenuated the inhibitory effect of EX-4 on H_2O_2-induced apoptosis (Fig. 3A), insulin secretion (Fig. 3B), and oxidative stress (Fig. 3C and D) in β-cells. However, silencing of TLR4 enhanced the effect of intervention with EX-4 in H_2O_2-induced β-cells (Fig. 3).

EX-4 inhibits oxidative stress in β-cells mediated by TLR4 or NF-κB. To confirm the effects of EX-4 on oxidative stress in β-cells mediated by TLR4 or NF-κB, the efficacy of EX-4 on the damage induced in β-cells using TLR4 agonists (LPS) or NF-κB agonists (TNF-α) was investigated. The results demonstrated that EX-4 decreased apoptosis (Fig. 4A and E), restored insulin secretion (Fig. 4B and F), and inhibited oxidative stress (Fig. 4C, D, G and H) in β-cells, which were injured by LPS or TNF-α.

Effects of EX-4 on HFD-induced oxidative stress in obese and $TLR4^{trun/trun}$ rats. The present study investigated the role of EX-4 in lipotoxicity-induced oxidative stress on obese rats induced with an HFD. The results uncovered that EX-4

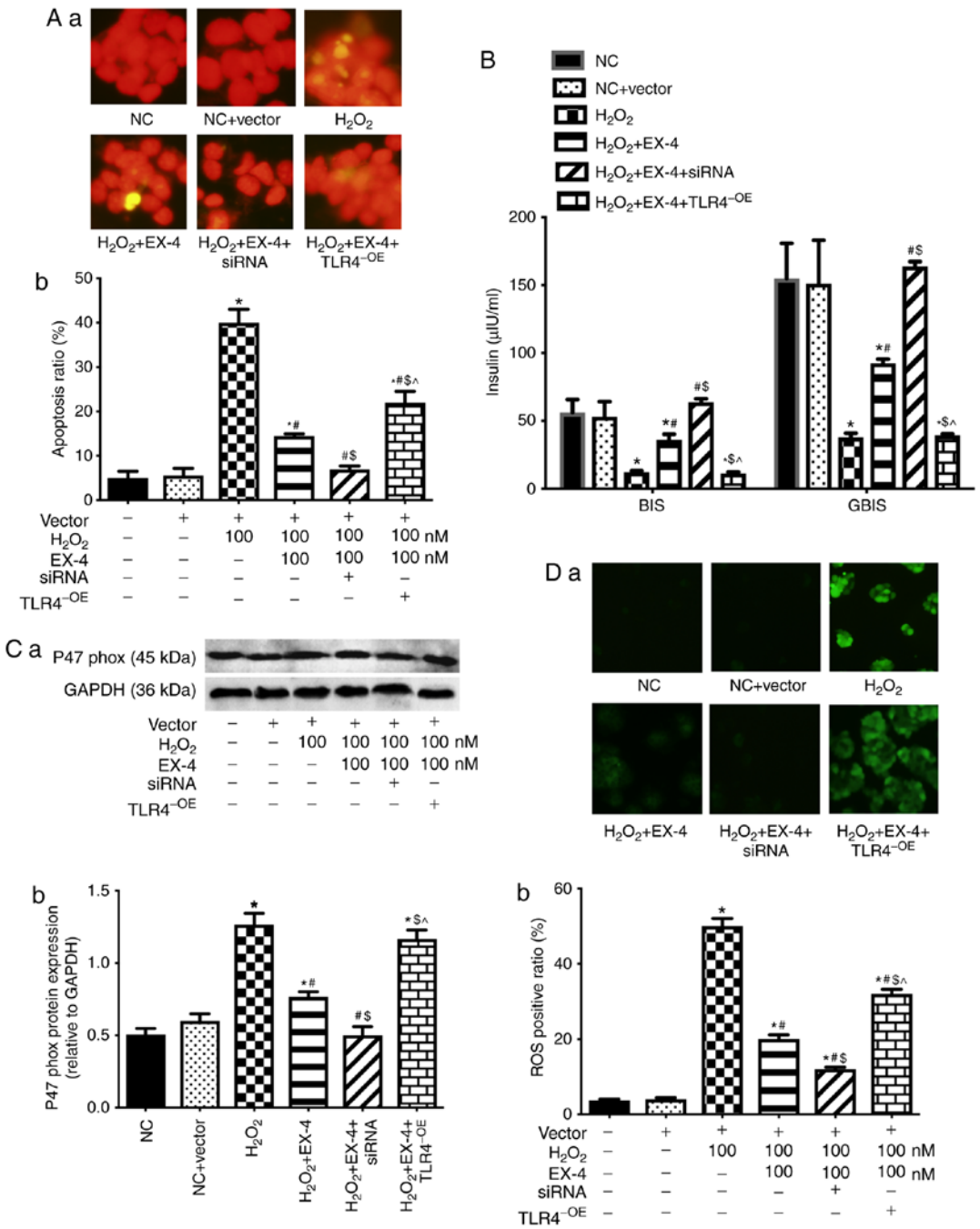

Figure 3. TLR4 is involved in the role of EX-4 in improving H_2O_2-induced oxidative stress in β-cells. (A) Apoptosis rate of β-cells. (A-a) Representative images from fluorescent microscopy in each group. (A-b) The collective analyses of all three independent experiments. (B) Insulin secretion. (C) Expression level of $p47^{phox}$. (C-a) Representative western blot images in each group. (C-b) The ratio of target protein to GAPDH. (D) Levels of ROS in β-cells. (D-a) Representative images from fluorescent microscopy in each group. (D-b) The collective analyses of all three independent experiments. $^{*}P<0.05$ vs. respective NC or vector group, $^{\#}P<0.05$ vs. H_2O_2 group, $^{\$}P<0.05$ vs. H_2O_2 + EX-4 group, $^{\wedge}P<0.05$ vs. H_2O_2 + EX-4 + siRNA group. Magnification, x40. NC, negative control; EX-4, exendin-4; siRNA, small interfering RNA; TLR4, toll-like receptor 4; OE, overexpression; BIS, basal insulin secretion; GSIS, glucose-stimulated insulin secretion; ROS, reactive oxygen species.

showed no significant effect on weight (Fig. 5A), the levels of TCHO, TG, LDL (Fig. 5B and C) or FFA (Fig. 5D), while it reduced Lee's index (Fig. 5E), HOMA-IR (Fig. 5F) and FBG (Fig. 5G), and increased insulin levels (Fig. 5H) in HFD rats. Besides, EX-4 inhibited the expression levels of TLR4, NF-κB p65 subunit and $p47^{phox}$ (Fig. 5I), decreased cell apoptosis (Fig. 5J) and the level of ROS (Fig. 5K), and rebalanced the α- to β-cell area ratio (α/β) in the pancreas (Fig. 5L).

To investigate the role of TLR4 in oxidative stress induced by a HFD, the TLR4 gene was truncated in rats. Compared with the wild-type with HFD group, truncation of TLR4 in the HFD group led to a decrease in weight (Fig. 5A), HOMA-IR (Fig. 5F), FBG (Fig. 5G), the expression levels of TLR4, NF-κB p65 subunit and $p47^{phox}$ (Fig. 5I), as well as the levels of cell apoptosis (Fig. 5J) and ROS in the pancreas (Fig. 5K), while rebalanced the α/β in pancreas (Fig. 5L). Simultaneously, compared with EX-4-treated wild-type obese rats, EX-4-treated

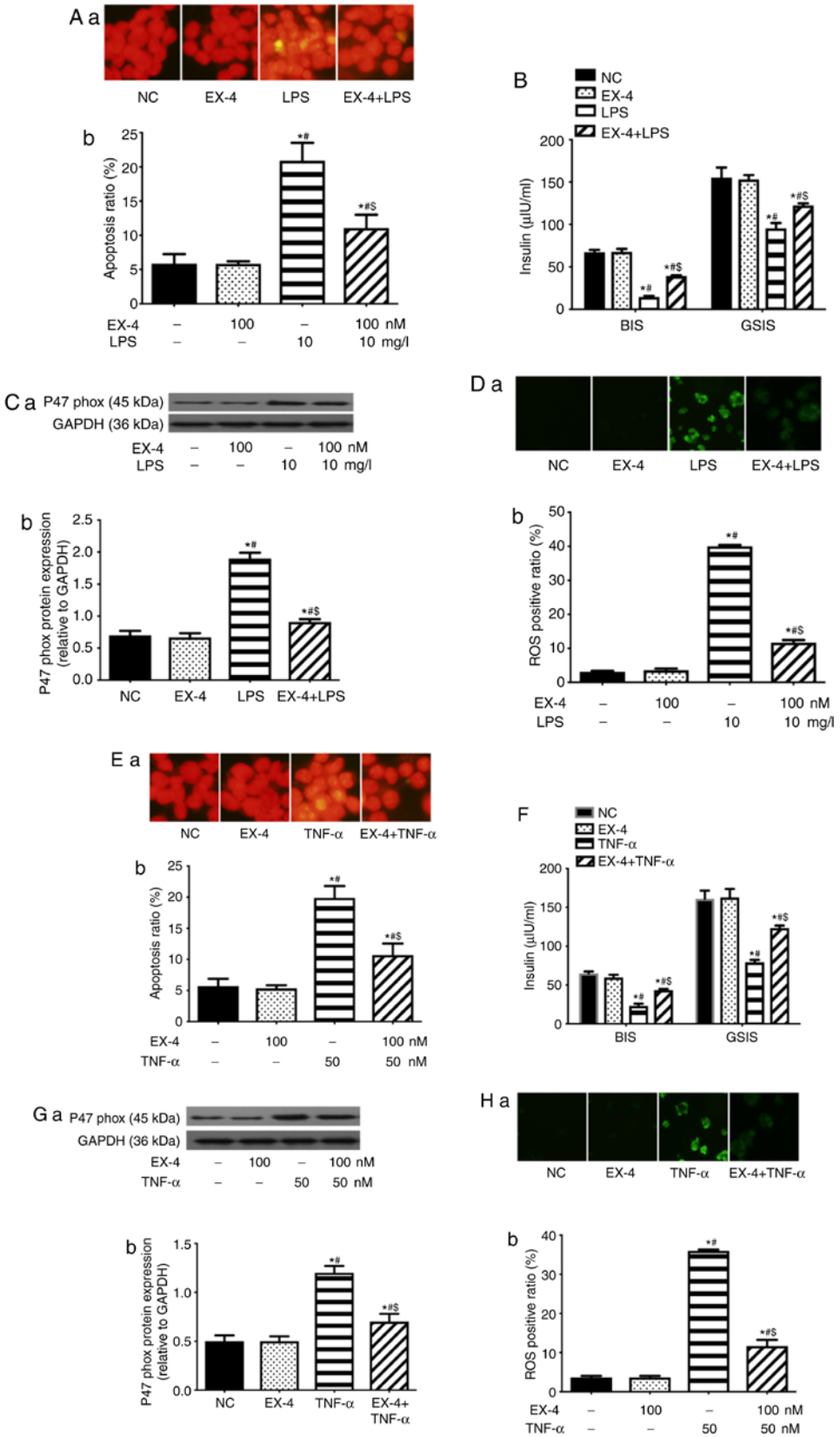

Figure 4. EX-4 inhibits TLR4 or NF-κB agonist-induced oxidative stress in β-cells. Exendin-4 inhibited TLR4 agonist induced oxidative stress in β-cells. (A) Apoptosis rate of β-cells. (A-a) Representative images from fluorescent microscopy in each group. (A-b) The collective analyses of all three independent experiments. (B) Insulin secretion. (C) Expression level of $p47^{phox}$. (C-a) Representative western blot images in each group. (C-b) The ratio of target protein to GAPDH. (D) Levels of ROS in β-cells. (D-a) Representative images from fluorescent microscopy in each group. (D-b) The collective analyses of all three independent experiments. EX-4 inhibited NF-κB agonist induced oxidative stress in β-cells. (E) Apoptosis rate of β-cells. (E-a) Representative images from fluorescent microscopy in each group. (E-b) The collective analyses of all three independent experiments. (F) Insulin secretion. (G) Expression level of $p47^{phox}$. (G-a) Representative western blot images in each group. (G-b) The ratio of target protein to GAPDH. (H) Levels of ROS in β-cells. (H-a) Representative images from fluorescent microscopy in each group. (H-b) The collective analyses of all three independent experiments. $^{*}P<0.05$ vs. NC group, $^{\#}P<0.05$ vs. EX-4 group and $^{\$}P<0.05$ vs. respective LPS or TNF-α group. Magnification, x40. NC, negative control; EX-4, exendin-4; LPS, lipopolysaccharide; ROS, reactive oxygen species; TNF-α, tumor necrosis factor-α; BIS, basal insulin secretion; GSIS, glucose-stimulated insulin secretion.

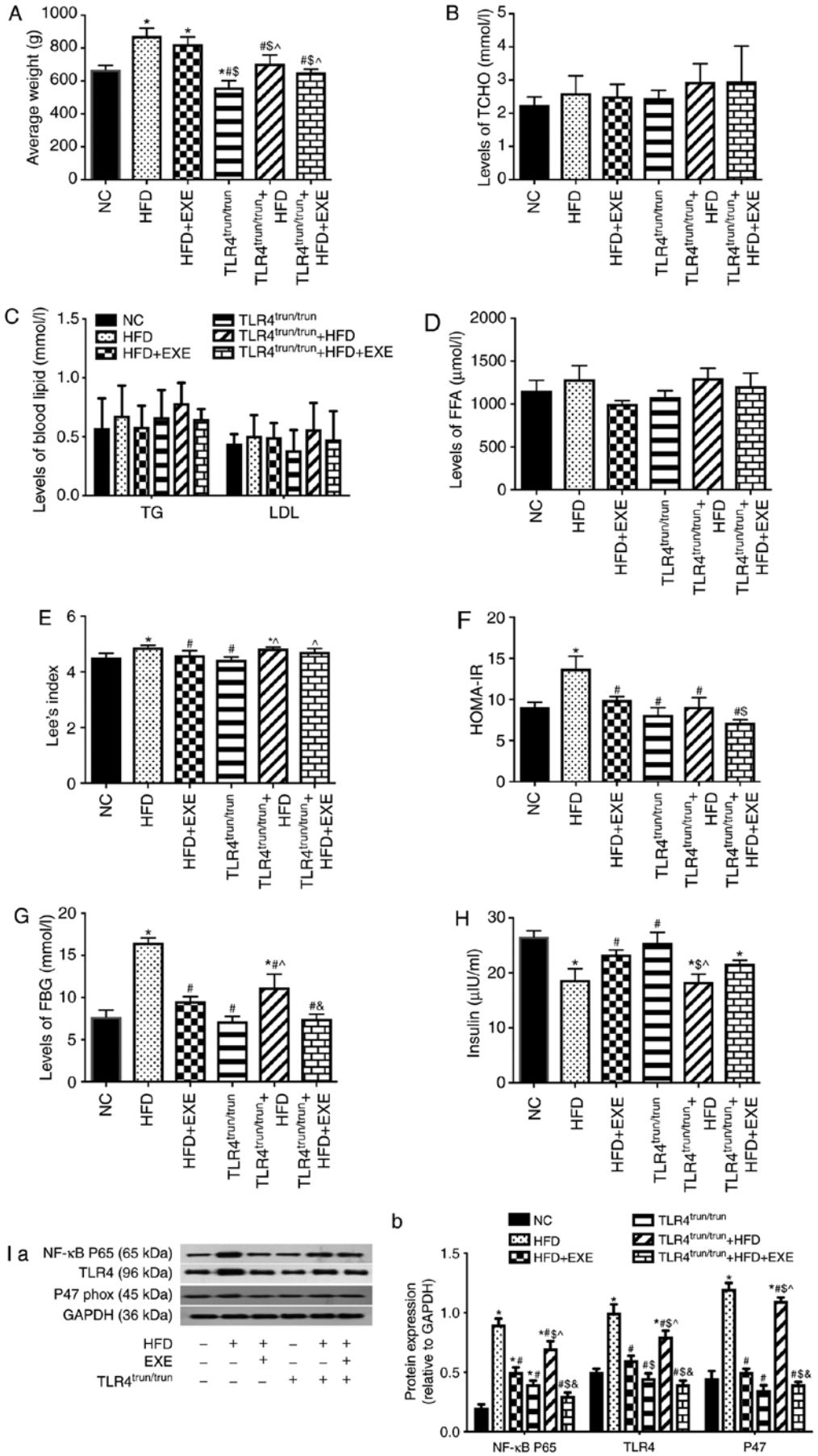

Figure 5. EXE alleviates islet oxidative stress in obese rats, and truncation of TLR4 attenuates the damage caused by a high-fat diet in synergy with EXE. (A) Average weight in each group. Levels of blood lipids were measured in each group: (B) TCHO, (C) TG and LDL, and (D) FFA. (E) Lee's index in each group. (F) HOMA-IR. (G) Levels of FBG. (H) Insulin levels. (I) Expression levels of NF-κB p65 subunit, TLR4 and $p47^{phox}$ in pancreatic tissues. (I-a) Representative western blot images in each group. (I-b) The ratio of target protein to GAPDH.

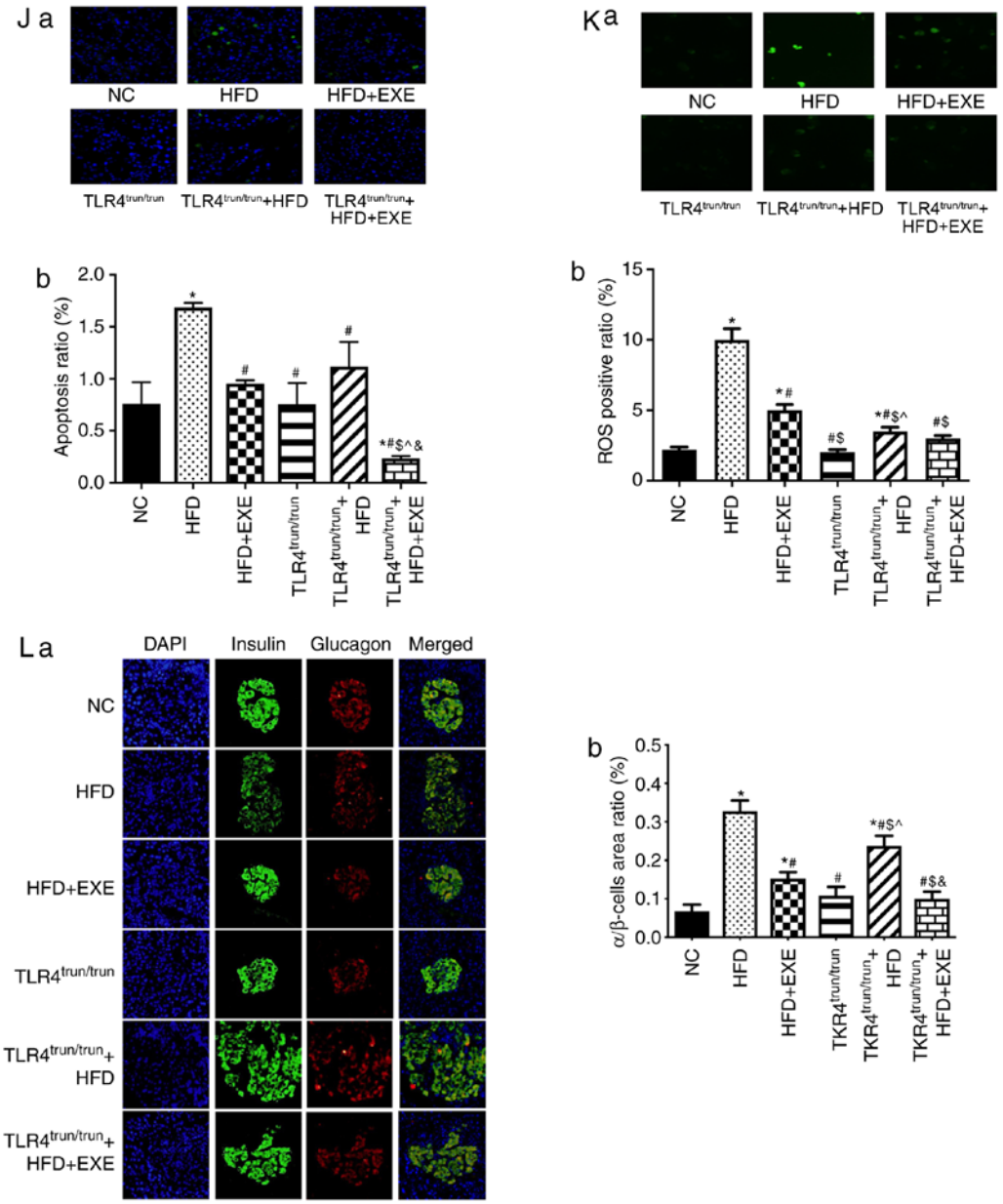

Figure 5. Continued. (J) Apoptosis in pancreatic tissue. (J-a) Representative images from fluorescent microscopy in each group. (J-b) The collective analyses of all three independent experiments. (K) The levels of ROS in pancreatic tissue. (K-a) Representative images from fluorescent microscopy in each group. (K-b) The collective analyses of all three independent experiments. (L) Immunofluorescence images of α- and β-cells in pancreatic tissues. (L-a) Representative images from fluorescent microscopy in each group. (L-b) The collective analyses of all three independent experiments. *P<0.05 vs. NC group, $^{\#}$P<0.05 vs. HFD group, $^{\$}$P<0.05 vs. HFD + EXE group, $^{\wedge}$P<0.05 vs. TLR4$^{trun/trun}$ group, $^{\&}$P<0.05 vs. TLR4$^{trun/trun}$ + HFD group. Magnification, x40. EXE, exenatide; TCHO, total cholesterol; FFA, free fatty acid; HOMA-IR, homeostatic model assessment of insulin resistance; FBG, fasting blood glucose; TG, triglyceride; LDL, low-density lipoprotein; HFD, high-fat diet; TLR4, toll-like receptor 4; trun, truncated.

TLR4 truncation of obese rats showed lower levels of weight (Fig. 5A), HOMA-IR (Fig. 5F), expression levels of TLR4, NF-κB p65 subunit and p47^{phox} (Fig. 5I), cell apoptosis (Fig. 5J), and the levels of ROS in the pancreas (Fig. 5K), and rebalanced the α/β in the pancreas (Fig. 5L).

Discussion

The present study used islet β-cells, obese SD rats and a TLR4 truncation rat model to observe the role and mechanism of EX-4 in lipotoxicity-induced oxidative stress in β-cells. The results revealed that EX-4 restrained PA-induced oxidative stress in β-cells and inhibited the expression levels of TLR4 and NF-κB p65 subunit in a concentration-dependent manner. Simultaneously, it was demonstrated that TLR4 was involved in the effects of EX-4 on suppressing H_2O_2-induced oxidative stress in β-cells. Moreover, EX-4 could inhibit TLR4- or NF-κB agonist-induced oxidative stress in β-cells. Furthermore, it was confirmed that in obese rats, EX-4 was able to reduce HOMA-IR, rebalance the distribution of α- or β-cells, and inhibit islet cell apoptosis, oxidative stress, and the expression levels of TLR4 and NF-κB p65 subunit. It was also confirmed that truncation of the TLR4 gene can delay the aforementioned damage induced by an HFD.

The current research disclosed that EX-4 had a direct impact on the suppression of oxidative stress in β-cells. To

date, animal and clinical trials have confirmed the intervention of EX-4 on vascular oxidative stress (29-31). Animal experiments have also demonstrated that liraglutide can increase the quality of β-cells by inhibiting oxidative stress and endoplasmic stress (32). It is noteworthy that $p47^{phox}$ is a major subunit of NADPH oxidase activity, whose activity influences the function of β-cells in human pancreatic islets (33). The aforementioned experiments also supported the present findings. However, the intervention of EX-4 on normal β-cells showed no influence on NADPH oxidase and ROS. It was hypothesized that NADPH oxidase and ROS are at very low levels under normal physiological conditions, and that changes caused by intervention with EX-4 may not be detectable.

At present, the pathway by which EX-4 inhibits oxidative stress in β-cells needs further study. Wu *et al* (34) reported that GLP-1 analogues can protect cardiac function by inhibiting the ROCK/peroxisome proliferator-activated receptor-α pathway to improve diabetic lipotoxic cardiomyopathy. A study showed that GLP-1 analogues may exert an effect on metabolic syndrome through a receptor-mediated mechanism (35). In the present study, it was found that EX-4 inhibited lipotoxicity-induced oxidative stress, and simultaneously the expression levels of TLR4 and NF-κB p65 subunit during the experimental process. Therefore, it was hypothesized that benign intervention with EX-4 was associated with inhibition of the expression levels of TLR4 and NF-κB p65 subunit. There are currently several clinical studies supporting this hypothesis. Ceriello *et al* (36) confirmed that GLP-1 analogues effectively improved endothelial dysfunction, and inhibited inflammation and oxidative stress in patients with type 2 diabetes. To further validate the hypothesis, the expression of TLR4 was altered in order to observe whether TLR4 was involved in the protective effect of EX-4 in inhibiting lipotoxicity-induced oxidative stress. The present results demonstrated that overexpression of TLR4 attenuated the effects of EX-4, while inhibition of TLR4 expression enhanced the influences of EX-4. These results were also confirmed when EX-4 was antagonized with H_2O_2-induced oxidative stress in β-cells. Moreover, EX-4 was able to inhibit TLR4 or NF-κB agonist-induced oxidative stress in β-cells. A previous study demonstrated the ability of EX-4 to inhibit NF-κB, and thus supported the present results (37). The results of the present study suggested that EX-4 could improve lipotoxicity-induced oxidative stress in β-cells by inhibiting the expression levels of TLR4 and NF-κB p65 subunit.

However, other studies have shown that GLP-1 analogues can act as a benign intervention in cardiomyocytes (38), the liver (39) and the kidney (40) by inhibiting inflammation or oxidative stress. To date, the antagonistic effect of GLP-1 analogues on inflammation and oxidative stress was also confirmed in β-cells (41). However, there is no direct evidence that GLP-1 inhibits oxidative stress by inhibiting the TLR4 signaling pathway. To further confirm the present results *in vitro*, HFD-induced obese SD rats were used, and it was confirmed that EX-4 can restrain lipotoxicity-induced insulin resistance, oxidative stress, and the expression levels of TLR4 and NF-κB p65 subunit. Furthermore, to investigate the role of TLR4 in lipotoxicity-induced oxidative stress and the effects of EX-4 on antagonizing the lipotoxicity, the TLR4 gene was truncated in rats. It was found that truncation of TLR4 amplified the effect of benign intervention with EX-4 on obese rats, confirming that EX-4 improved hyperlipidemia-induced oxidative stress by inhibiting the TLR4 pathway. Although the protective effects of EX-4 in the $TLR4^{trun/trun}$ group were significantly lower than those in wild-type group, there was no significant difference between $TLR4^{trun/trun}$ HFD group and $TLR4^{trun/trun}$ normal diet. This is due to the substantial role of TLR4 in hyperlipidemia-induced oxidative stress, and truncation of TLR4 can significantly inhibit the damage induced by an HFD; besides, EX-4 showed a protective effect, mainly by suppressing TLR4. Therefore, treatment with EX-4 led to no significant differences in rats with truncation of the TLR4 gene.

The results of the present study revealed that EX-4 had no significant influence on weight; however, several previously published studies showed the opposite effect (7,41-43). It is speculated that the inconsistent results may be due to different intervention time periods. The time recorded in the aforementioned research papers was between 24 h and 3 weeks, and the intervention time in the present study was 16 weeks. It was found that EX-4 can reduce the BW of obese rats over the course of 4 weeks, while the weight was regained in obese rats with a more prolonged duration of intervention (Fig. S3). Thus, it was hypothesized that obese rats would show resistance to EX-4 as the intervention time was prolonged. To date, a study has supported long-term intervention with EX-4 for reducing weight in obese individuals (44).

In addition, the results of the present study demonstrated that TLR4 protein is still expressed in truncation rats, possibly due to the fact that the CRISPR/Cas9 system was used for the TLR4 truncation (-178 bp +7 bp; exon -149 bp; Data S1), without knocking out TLR4 DNA. The TLR4 protein was detected in TLR4 truncation rats using western blot analysis, and the molecular weight of TLR4 in TLR4 truncation rats was similar to that in wild-type rats. It was speculated that this might be due to the lack of specificity of the TLR4 antibody. Therefore, RT-sqPCR was used to detect TLR4 mRNA expression, and it was found that TLR4 had a length of 436 bp in truncation rats, demonstrating that the truncation of the gene was successfully carried out (Fig. S4).

The present study showed that EX-4 decreased lipotoxicity-induced insulin resistance, oxidative stress, and the expression levels of TLR4 and NF-κB p65 subunit. Previous studies have demonstrated that GLP-1 analogues can decrease the weight of obese patients (45), reduce insulin resistance (46) and improve islet function (47). However, obese patients are characterized by uncertain resistance to GLP-1 analogues, which weakens the effectiveness of GLP-1 analogues in obese patients compared with those of average weight (48). Therefore, the use of GLP-1 as a drug for preventing diabetes in obese patients should be further studied. Simultaneously, due to the benefits of TLR4 in mediating metabolic inflammation and oxidative stress induced by hyperlipidemia, TLR4 inhibitors could be used as potential weight-loss drugs. Furthermore, the present results provide an experimental basis for anti-inflammatory treatment in obese patients to prevention of diabetes. However, the present study contains certain limitations. Firstly, the mechanism of action EX-4 on TLR4 was not confirmed, and the direct or indirect interactions between the two require further research. Secondly, the relationship between the protective effects of EX-4 and GLP-1 analogues was not observed. Further research is therefore essential to

confirm the clinical data. Thirdly, the effects of blood glucose fluctuations on the model animal in the present study were not assessed. To control for the effects of blood glucose, covariance analysis was used to investigate the effect of exenatide on the model animals. It was found that exenatide inhibited HFD-induced oxidative stress in β-cells, independent of blood glucose fluctuations (Table SII). Lastly, βTC6 is a mouse islet cell line and does not fully represent islet β cells.

In conclusion, it was found that EX-4 can inhibit damage caused by lipotoxicity-induced oxidative stress in β-cells through suppression of the TLR4/NF-κB signaling pathway. The present study revealed a new mechanism by which EX-4 may inhibit lipotoxicity-induced oxidative stress in β-cells, providing experimental evidence for TLR4 as a therapeutic target in weight loss and for treating oxidative stress in β-cells.

Acknowledgements

Not applicable.

Funding

This study was supported by Science and Technology Innovation Joint Fund Project Fujian Province (grant no. 2016Y9102), Grants from National Natural Science Foundation of China (grant nos. 81500632 and 81870572), Natural Science Foundation of Fujian Province (grant nos. 2019J01455 and 2015J01453), Fujian Province Higher Education Institute New Century Research Project (grant no. 2018B049), and the Medical Innovation Fund Project of Fujian Province (grant no. 2018-CX-23).

Availability of data and materials

All data generated or analyzed during this study are included in this published article.

Authors' contributions

XS made substantial contributions to the conception and design of the study, and was involved in drafting the manuscript and revising it critically for important intellectual content; LY designed the study and reviewed/edited the drafts, and is guarantor; LL and MY were involved in the acquisition of data and drafting the manuscript; YL and JL were involved in the interpretation of data and drafting the manuscript. LY is the guarantor of this work. All authors took responsibility for the integrity of the data and the accuracy of the data analysis and have given final approval of the version to be published and agreed to be accountable for all aspects of the work.

Ethics approval and consent to participate

The study was approved by the Biomedical Research Ethics Committee of the First Affiliated Hospital of Fujian Medical University.

Patient consent for publication

Not applicable.

Competing interests

The authors declare that they have no competing interests.

References

1. Hirota Y, Matsuda T, Nakajima S, Takabe M, Hashimoto N, Nakamura T, Okada Y, Sakaguchi K and Ogawa W: Effects of exenatide and liraglutide on postchallenge glucose disposal in individuals with normal glucose tolerance. Endocrine 64: 43-47, 2019.
2. Gu J, Wei Q, Zheng H, Meng X, Zhang J and Wang D: Exendin-4 promotes survival of mouse pancreatic beta-cell line in lipotoxic conditions, through the extracellular signal-related kinase 1/2 pathway. J Diabetes Res 2016: 5294025, 2016.
3. Natalicchio A, Labarbuta R, Tortosa F, Biondi G, Marrano N, Peschechera A, Carchia E, Orlando MR, Leonardini A, Cignarelli A, *et al*: Exendin-4 protects pancreatic beta cells from palmitate-induced apoptosis by interfering with GPR40 and the MKK4/7 stress kinase signalling pathway. Diabetologia 56: 2456-2466, 2013.
4. Oh YS, Lee YJ, Kang Y, Han J, Lim OK and Jun HS: Exendin-4 inhibits glucolipotoxic ER stress in pancreatic β cells via regulation of SREBP1c and C/EBPβ transcription factors. J Endocrinol 216: 343-352, 2013.
5. Wu X, Liang W, Guan H, Liu J, Liu L, Li H, He X, Zheng J, Chen J, Cao X and Li Y: Exendin-4 promotes pancreatic β-cell proliferation via inhibiting the expression of Wnt5a. Endocrine 55: 398-409, 2017.
6. Natalicchio A, Biondi G, Marrano N, Labarbuta R, Tortosa F, Spagnuolo R, D'Oria R, Carchia E, Leonardini A, Cignarelli A, *et al*: Long-term exposure of pancreatic β-cells to palmitate results in SREBP-1C-dependent decreases in GLP-1 receptor signaling via CREB and AKT and insulin secretory response. Endocrinology 157: 2243-2258, 2016.
7. Yang Y, Choi PP, Smith WW, Xu W, Ma D, Cordner ZA, Liang NC and Moran TH: Exendin-4 reduces food intake via the PI3K/AKT signaling pathway in the hypothalamus. Sci Rep 7: 6936, 2017.
8. Iwasaki S, Hamada T, Chisaki I, Andou T, Sano N, Furuta A and Amano N: Mechanism-based pharmacokinetic/pharmacodynamic modeling of the glucagon-like peptide-1 receptor agonist exenatide to characterize its antiobesity effects in diet-induced obese mice. J Pharmacol Exp Ther 362: 441-449, 2017.
9. Dandona P, Ghanim H, Abuaysheh S, Green K, Dhindsa S, Makdissi A, Batra M, Kuhadiya ND and Chaudhuri A: Exenatide increases IL-1RA concentration and induces Nrf-2Keap-1regulated antioxidant enzymes: Relevance to β-cell function. J Clin Endocrinol Metab 103: 1180-1187, 2018.
10. Varin EM, Wojtusciszyn A, Broca C, Muller D, Ravier MA, Ceppo F, Renard E, Tanti JF and Dalle S: Inhibition of the MAP3 kinase Tpl2 protects rodent and human β-cells from apoptosis and dysfunction induced by cytokines and enhances anti-inflammatory actions of exendin-4. Cell Death Dis 7: e2065, 2016.
11. Chang G, Liu J, Qin S, Jiang Y, Zhang P, Yu H, Lu K, Zhang N, Cao L, Wang Y, *et al*: Cardioprotection by exenatide: A novel mechanism via improving mitochondrial function involving the GLP-1 receptor/cAMP/PKA pathway. Int J Mol Med 41: 1693-1703, 2018.
12. Kawaguchi T, Itou M, Taniguchi E and Sata M: Exendin4, a glucagonlike peptide1 receptor agonist, modulates hepatic fatty acid composition and Δ-5desaturase index in a murine model of nonalcoholic steatohepatitis. Int J Mol Med 34: 782-787, 2014.
13. Lee SM, Choi SE, Lee JH, Lee JJ, Jung IR, Lee SJ, Lee KW and Kang Y: Involvement of the TLR4 (Toll-like receptor4) signaling pathway in palmitate-induced INS-1 beta cell death. Mol Cell Biochem 354: 207-217, 2011.
14. Eguchi K, Manabe I, Oishi-Tanaka Y, Ohsugi M, Kono N, Ogata F, Yagi N, Ohto U, Kimoto M, Miyake K, *et al*: Saturated fatty acid and TLR signaling link β cell dysfunction and islet inflammation. Cell Metab 15: 518-533, 2012.
15. Wang X, Ge QM, Bian F, Dong Y and Huang CM: Inhibition of TLR4 protects rat islets against lipopolysaccharide-induced dysfunction. Mol Med Rep 15: 805-812, 2017.
16. Shen X, Yang L, Yan S, Zheng H, Liang L, Cai X and Liao M: Fetuin A promotes lipotoxicity in β cells through the TLR4 signaling pathway and the role of pioglitazone in anti-lipotoxicity. Mol Cell Endocrinol 412: 1-11, 2015.

17. Ma C, Jiang Y, Zhang X, Chen X, Liu Z and Tian X: Isoquercetin ameliorates myocardial infarction through anti-inflammation and anti-apoptosis factor and regulating TLR4-NF-kB signal pathway. Mol Med Rep 17: 6675-6680, 2018.
18. Zhou Y, Ding YL, Zhang JL, Zhang P, Wang JQ and Li ZH: Alpinetin improved high fat diet-induced non-alcoholic fatty liver disease (NAFLD) through improving oxidative stress, inflammatory response and lipid metabolism. Biomed Pharmacother 97: 1397-1408, 2018.
19. Xu MX, Wang M and Yang WW: Gold-quercetin nanoparticles prevent metabolic endotoxemia-induced kidney injury by regulating TLR4/NF-κB signaling and Nrf2 pathway in high fat diet fed mice. Int J Nanomedicine 12: 327-345, 2017.
20. Xiang JN, Chen DL and Yang LY: Effect of PANDER in βTC6-cell lipoapoptosis and the protective role of exendin-4. Biochem Biophys Res Commun 421: 701-706, 2012.
21. Kondo M, Tanabe K, Amo-Shiinoki K, Hatanaka M, Morii T, Takahashi H, Seino S, Yamada Y and Tanizawa Y: Activation of GLP-1 receptor signalling alleviates cellular stresses and improves beta cell function in a mouse model of Wolfram syndrome. Diabetologia 61: 2189-2201, 2018.
22. Yang G, Lei Y, Inoue A, Piao L, Hu L, Jiang H, Sasaki T, Wu H, Xu W, Yu C, *et al*: Exenatide mitigated diet-induced vascular aging and atherosclerotic plaque growth in ApoE-deficient mice under chronic stress. Atherosclerosis 264: 1-10, 2017.
23. Ke J, Wei R, Yu F, Zhang J and Hong T: Liraglutide restores angiogenesis in palmitate-impaired human endothelial cells through PI3K/Akt-Foxo1-GTPCH1 pathway. Peptides 86: 95-101, 2016.
24. Shen X, Yang L, Yan S, Wei W, Liang L, Zheng H and Cai X: The effect of FFAR1 on pioglitazone-mediated attenuation of palmitic acid-induced oxidative stress and apoptosis in βTC6 cells. Metabolism 63: 335-351, 2014.
25. Seo JH, Lim JW and Kim H: Differential role of ERK and p38 on NF-κB activation in helicobacter pylori-infected gastric epithelial cells. J Cancer Prev 18: 346-350, 2013.
26. Lu Z, Shen SX, Zhi DJ and Luo FH: The establishment of 'two-step sequential filtration method' on the yield rate of purified islets in rats. Zhongguo Dang Dai Er Ke Za Zhi 15: 572-576, 2013 (In Chinese).
27. Kassem M, Niazi ZR, Abbas M, El Habhab A, Kreutter G, Khemais-Benkhiat S, Auger C, Antal MC, Schini-Kerth VB, Toti F and Kessler L: Senescence of pancreas in middle-aged rats with normal vascular function. Ann Transplant 22: 177-186, 2017.
28. Chen DL, Xiang JN and Yang LY: Role of ERp46 in β-cell lipoapoptosis through endoplasmic reticulum stress pathway as well as the protective effect of exendin-4. Biochem Biophys Res Commun 426: 324-329, 2012.
29. Li Q, Lin Y, Wang S, Zhang L and Guo L: GLP-1 inhibits high-glucose-induced oxidative injury of vascular endothelial cells. Sci Rep 7: 8008, 2017.
30. Schiapaccassa A, Maranhão PA, de Souza MDGC, Panazzolo DG, Nogueira Neto JF, Bouskela E and Kraemer-Aguiar LG: 30-days effects of vildagliptin on vascular function, plasma viscosity, inflammation, oxidative stress, and intestinal peptides on drug-naive women with diabetes and obesity: A randomized head-to-head metformin-controlled study. Diabetol Metab Syndr 11: 70, 2019.
31. Steven S, Jurk K, Kopp M, Kröller-Schön S, Mikhed Y, Schwierczek K, Roohani S, Kashani F, Oelze M, Klein T, *et al*: Glucagon-like peptide-1 receptor signalling reduces microvascular thrombosis, nitro-oxidative stress and platelet activation in endotoxaemic mice. Br J Pharmacol 174: 1620-1632, 2017.
32. Shimoda M, Kanda Y, Hamamoto S, Tawaramoto K, Hashiramoto M, Matsuki M and Kaku K: The human glucagon-like peptide-1 analogue liraglutide preserves pancreatic beta cells via regulation of cell kinetics and suppression of oxidative and endoplasmic reticulum stress in a mouse model of diabetes. Diabetologia 54: 1098-1108, 2011.
33. Rebelato E, Mares-Guia TR, Graciano MF, Labriola L, Britto LR, Garay-Malpartida HM, Curi R, Sogayar MC and Carpinelli AR: Expression of NADPH oxidase in human pancreatic islets. Life Sci 91: 244-249, 2012.
34. Wu L, Wang K, Wang W, Wen Z, Wang P, Liu L and Wang DW: Glucagon-like peptide-1 ameliorates cardiac lipotoxicity in diabetic cardiomyopathy via the PPARα pathway. Aging Cell 17: e12763, 2018.
35. Tesauro M, Schinzari F, Adamo A, Rovella V, Martini F, Mores N, Barini A, Pitocco D, Ghirlanda G, Lauro D, *et al*: Effects of GLP-1 on forearm vasodilator function and glucose disposal during hyperinsulinemia in the metabolic syndrome. Diabetes Care 36: 683-689, 2013.
36. Ceriello A, Novials A, Canivell S, La Sala L, Pujadas G, Esposito K, Testa R, Bucciarelli L, Rondinelli M and Genovese S: Simultaneous GLP-1 and insulin administration acutely enhances their vasodilatory, antiinflammatory, and antioxidant action in type 2 diabetes. Diabetes Care 37: 1938-1943, 2014.
37. Liu XH, Wang YP, Wang LX, Chen Z, Liu XY and Liu LB: Exendin-4 protects murine MIN6 pancreatic β-cells from interleukin-1β-induced apoptosis via the NF-κB pathway. J Endocrinol Invest 36: 803-811, 2013.
38. Chang G, Zhang D, Yu H, Zhang P, Wang Y, Zheng A and Qin S: Cardioprotective effects of exenatide against oxidative stress-induced injury. Int J Mol Med 32: 1011-1020, 2013.
39. Gao H, Zeng Z, Zhang H, Zhou X, Guan L, Deng W and Xu L: The glucagon-like peptide-1 analogue liraglutide inhibits oxidative stress and inflammatory response in the liver of rats with diet-induced non-alcoholic fatty liver disease. Biol Pharm Bull 38: 694-702, 2015.
40. Tanaka T, Higashijima Y, Wada T and Nangaku M: The potential for renoprotection with incretin-based drugs. Kidney Int 86: 701-711, 2014.
41. Kim MH, Kim EH, Jung HS, Yang D, Park EY and Jun HS: EX4 stabilizes and activates Nrf2 via PKCδ, contributing to the prevention of oxidative stress-induced pancreatic beta cell damage. Toxicol Appl Pharmacol 315: 60-69, 2017.
42. Kanoski SE, Hayes MR and Skibicka KP: GLP-1 and weight loss: Unraveling the diverse neural circuitry. Am J Physiol Regul Integr Comp Physiol 310: R885-R895, 2016.
43. Wolak M, Staszewska T, Juszczak M, Gałdyszyńska M and Bojanowska E: Anti-inflammatory and pro-healing impacts of exendin-4 treatment in Zucker diabetic rats: Effects on skin wound fibroblasts. Eur J Pharmacol 842: 262-269, 2019.
44. Basolo A, Burkholder J, Osgood K, Graham A, Bundrick S, Frankl J, Piaggi P, Thearle MS and Krakoff J: Exenatide has a pronounced effect on energy intake but not energy expenditure in non-diabetic subjects with obesity: A randomized, double-blind, placebo-controlled trial. Metabolism 85: 116-125, 2018.
45. Jorsal T, Rungby J, Knop FK and Vilsbøll T: GLP-1 and amylin in the treatment of obesity. Curr Diab Rep 16: 1, 2016.
46. Camastra S, Astiarraga B, Tura A, Frascerra S, Ciociaro D, Mari A, Gastaldelli A and Ferrannini E: Effect of exenatide on postprandial glucose fluxes, lipolysis, and β-cell function in non-diabetic, morbidly obese patients. Diabetes Obes Metab 19: 412-420, 2017.
47. Sun XF, Wang Y, Zhao WJ, Wang L, Bao DQ, Qu GR, Yao MX, Luan J, Wang YG and Yan SL: Effect of liraglutide on glucagon secretion in obese type 2 diabetic patients. Zhonghua Nei Ke Za Zhi 58: 33-38, 2019 (In Chinese; Abstract available in Chinese from the publisher).
48. Opinto G, Natalicchio A and Marchetti P: Physiology of incretins and loss of incretin effect in type 2 diabetes and obesity. Arch Physiol Biochem 119: 170-178, 2013.